JOURNAL OF SYNCHROTRON RADIATION

ISSN 1600-5775

Received 15 September 2016
Accepted 12 February 2017

Edited by D. A. Reis, SLAC National Accelerator Laboratory, USA

Keywords: acceleration time dilation; Mössbauer spectrum.

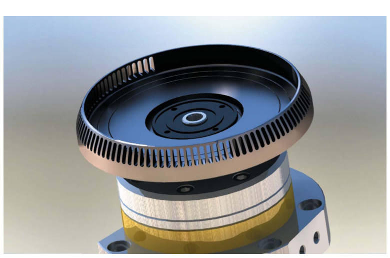

Advances in testing the effect of acceleration on time dilation using a synchrotron Mössbauer source

Y. Friedman,[a]* I. Nowik,[b] I. Felner,[b] J. M. Steiner,[a] E. Yudkin,[a] S. Livshitz,[a] H.-C. Wille,[c] G. Wortmann[d] and A. I. Chumakov[e]

[a]Jerusalem College of Technology, POB 16031, Jerusalem 91160, Israel, [b]Racah Institute of Physics, Hebrew University, Jerusalem 91904, Israel, [c]Deutsches Elektronen-Synchrotron, Notkestrasse 85, D-22607 Hamburg, Germany, [d]Department Physik, Universität Paderborn, Warburger Strasse 100, D-33098 Paderborn, Germany, and [e]European Synchrotron Radiation Facility, BP 220, F-38043 Grenoble, France. *Correspondence e-mail: friedman@jct.ac.il

New results, additional techniques and know-how acquired, developed and employed in a recent HC-1898 experiment at the Nuclear Resonance Beamline ID18 of ESRF are presented, in the quest to explore the acceleration effect on time dilation. Using the specially modified Synchrotron Mössbauer Source and KB-optics together with a rotating single-line semicircular Mössbauer absorber on the rim of a specially designed rotating disk, the aim was to measure the relative spectral shift between the spectra of two states when the acceleration of the absorber is anti-parallel and parallel to the source. A control system was used for the first time and a method to quantify the effects of non-random vibrations on the spectral shift was developed. For several runs where the effect of these vibrations was negligible, a stable statistically significant non-zero relative shift was observed. This suggests the influence of acceleration on time.

1. Introduction

Einstein's theory of Special Relativity (Einstein, 1905) predicts a time dilation of a moving object depending on the velocity of the object. Since time is directly connected to frequency, the frequency absorption spectrum of a uniformly rotating absorber will be shifted concurring with this time dilation. For regular velocities this shift is very small, so one needs very accurate means to measure it. After the discovery of the Mössbauer effect in 1958, several experiments, including Kündig's ingenious experiment (Kündig, 1963), used a rotating Mössbauer absorber to test the validity of Einstein's time dilation formula.

The question arises: 'Is there an additional time dilation due to the acceleration of the absorber?' According to Einstein's Clock Hypothesis (Einstein, 1911) the rate of an accelerated clock is equal to that of a co-moving unaccelerated clock. If acceleration also influences time, the existence of a maximal acceleration a_m (Friedman & Gofman, 2010) and a Doppler type shift due to acceleration (Friedman, 2011) were predicted. This Doppler type shift is similar to that due to the velocity, with velocity and maximal velocity replaced with acceleration and maximal acceleration, respectively. Since rotating Mössbauer absorbers are exposed to centripetal acceleration, they can also be used to test the effect of acceleration on time dilation.

Even nowadays, the absorption spectral lines are usually obtained by placing the Mössbauer source on a transducer. For technical reasons, it is very complicated to keep the balance of a fast rotating disk with moving parts on it. Thus, one is forced to have the transducer outside the rotating disk. In this case it was claimed (Friedman & Nowik, 2012) and confirmed experimentally (Friedman *et al.*, 2015) that, for a source outside the rotating disk, the absorption line of a rotating Mössbauer absorber is broadened during the rotation and that this broadening is linearly proportional to the rotation frequency. This necessitates the use of a strong Mössbauer source with the capability to be focused to the center of the disk. The Synchrotron Mössbauer Source (SMS) (Potapkin *et al.*, 2012) at the Nuclear Resonance Beamline ID18 (Rüffer & Chumakov, 1996) of ESRF together with the KB-optics (Kirkpatrick & Baez, 1948) to focus this beam was the ideal choice for our experiments.

During July 2014, Friedman *et al.* performed experiment HC-1361 at beamline ID18 at ESRF and obtained for the first time the *entire resonant line* of a rotating absorber. This experiment revealed (Friedman *et al.*, 2015) that, in this setup, this line was shifted by the so-called *alignment shift* (AS) due to the longitudinal Doppler shift between the SMS beam and the rotating absorber at the point of incidence.

For any single incident ray of the beam (parallel or not to the x-axis), we denote by $d = |\overline{OF}|$ the distance from the ray to the axis of rotation. The magnitude of the velocity of the absorber at the point of incidence A is $v = \omega r_{\rm a}$, where ω is the rotation frequency and $r_{\rm a} = |OA|$. This velocity $\mathbf{v}$ is perpendicular to OA. We decompose $\mathbf{v}$ into its parallel and transverse components $\mathbf{v}_{\parallel}$ and $\mathbf{v}_{\perp}$ relative to the incident ray, respectively (see Fig. 1). Since $\angle ACE = \angle OAF$, then $v_{\parallel} = \omega r_{\rm a} \sin\varphi = \omega r_{\rm a}(d/r_{\rm a}) = \omega d$. Thus, since $v_{\parallel}$ depends on d and ω *only*, for any given ray, this parallel component is identical for both points of incidence A and B. Hence, the AS of the beam, obtained by averaging over the whole conglomerate of rays, will be the same at both points of incidence.

As suggested by Friedman (2013), our experiment uses a semicircular absorber, and, in the same run, we separate the absorption data into *two states* (a) and (b) when the acceleration a is anti-parallel and parallel to the SMS radiation, with points of incidence **A** and **B**, respectively (see Fig. 2). The absorption lines for each state are affected by the same AS, and consequently their difference, called the *relative shift*, is not affected by the AS.

Based on the experiences of this experiment, a follow-up improved experiment HC-1898 was performed in July 2015 at the same facility. In this paper we present the additional techniques employed to improve the experiment, the know-how we acquired during this experiment, together with the findings of the experiment. We discovered that one must also consider the significant effect of the periodic non-random vibrations of the rotor/bearing system on the spectral shift. Even after taking into account the effect of these vibrations, for several runs where the effect of these vibrations was negligible we nevertheless observed a stable statistically significant non-zero relative shift.

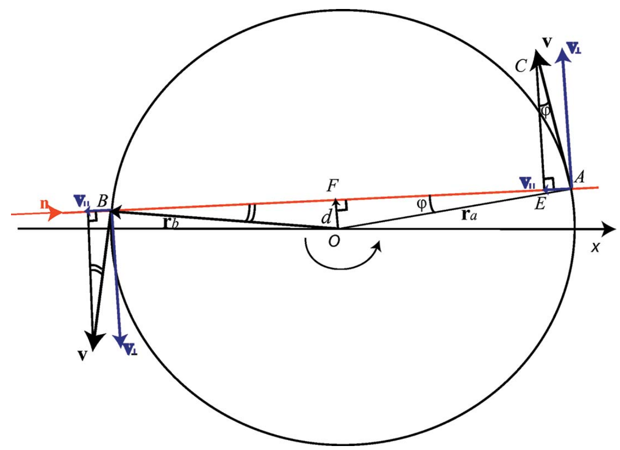

Figure 1
Velocity decomposition of a rotating absorber relative to an incident ray.

Since the spectra for each of the states (a) and (b) are obtained by using the same SMS source, the same Mössbauer absorber, and are equally affected by the velocity of the absorber with respect to the source, should the acceleration not influence time (frequency), these two spectra should be *identical*. The observed relative shift between the spectra of these states suggests that *the acceleration influences the time dilation*.

2. Additional improvements and know-how

The basic experimental setup comprising the specially designed high-speed air-bearing rotor (produced by Colibri Spindles Ltd, Israel), SMS and KB-optics was identical to the one used in the previous experiment HC-1361 (Friedman *et al.*, 2015). However, in order to increase significantly the count rate, the stainless-steel Mössbauer absorber used previously was replaced by a 95% enriched ^{57}Fe potassium ferrocyanide $K_4Fe(CN)_6{\cdot}3H_2O$ single-line absorber. The effect of the Mössbauer absorption line (at very low rotation) was 0.75

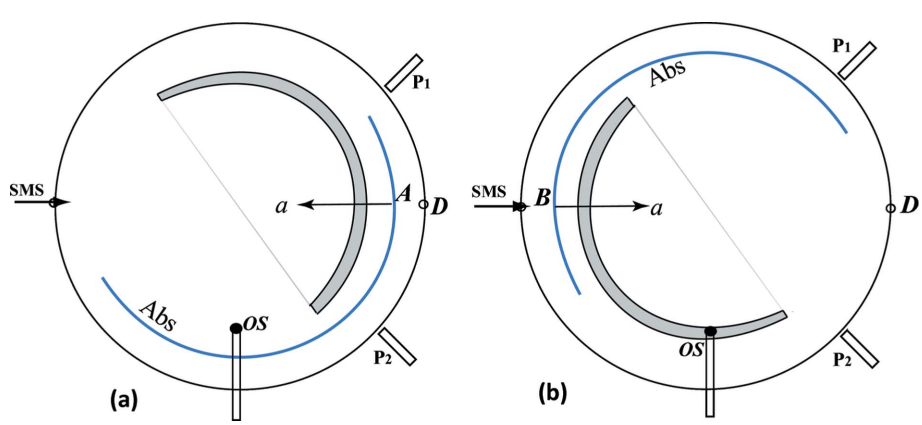

Figure 2
Setup and two states (a) and (b), SMS source, semicircular absorber (Abs), optical sensor (OS), proximity sensors (P_1, P_2) and detector (D).

(75%) and the half-width half-height parameter γ = 0.33 mm s^{-1}. Moreover, in order to narrow the rotational broadening of the resonant lines by blocking the peripheral rays of the beam and thus obtain spectra at higher rotation frequencies, the non-adjustable Re metal slit used previously was replaced by a gold-plated adjustable (four degrees of freedom) slit placed above the axis of rotation of the disk outside the vacuum chamber. Finally, in order to provide on-line information on the vibrations of the disk, an electronic computerized control system comprising two proximity sensors and an optical sensor was implemented.

While performing the experiment with these improvements, we acquired important additional know-how, such as: (i) how to align initially the beam to the center of the disk using a horizontal scan of the rotating disk, (ii) how to narrow the broadening of the resonant lines caused by the rotation, (iii) how to monitor vibrations using the control system, and a method (iv) how to quantify the effects of the non-random vibrations on the spectral shift. The technique we used to monitor the vibrations and the method we devised to quantify the effect of the non-random vibrations on the observed relative shift are presented in detail elsewhere (Friedman *et al.*, 2016).

The fundamental requirement for this experiment is that the beam should be focused to the axis of rotation. In our previous experiment we found a way to align the center of the beam to the axis of rotation by using the formula for the AS [Friedman *et al.*, 2016, formula (7)] for the dependence of the observed spectral shift with the distance from the center of the beam to the axis of rotation. However, in order to initiate this alignment process one must bring the Mössbauer resonant line (shifted by AS) inside the (narrow) observed frequencies window, a task which is cumbersome to achieve by trial and error.

In this experiment we found a fast technique to obtain an *initial alignment* of the system which does not require the use of SMS, hence it can be used also for other applications. This technique aligns the center of the beam to the center of the disk rather than to the axis of rotation. This was sufficient for our experiment since the center of the disk is only a few micrometers away from the axis of rotation. For the initial alignment we used the fact that our disk has diametrically aligned identical slots separated by non-transparent walls on its rim (see Fig. 3).

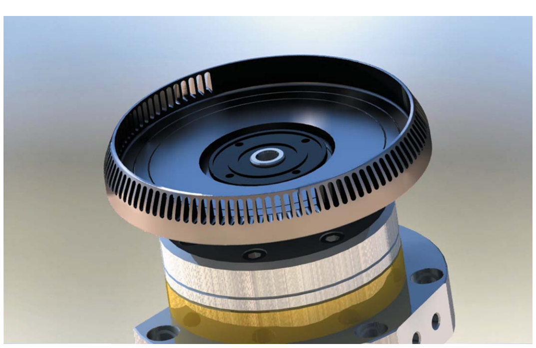

Figure 3
The disk with the slots and absorber.

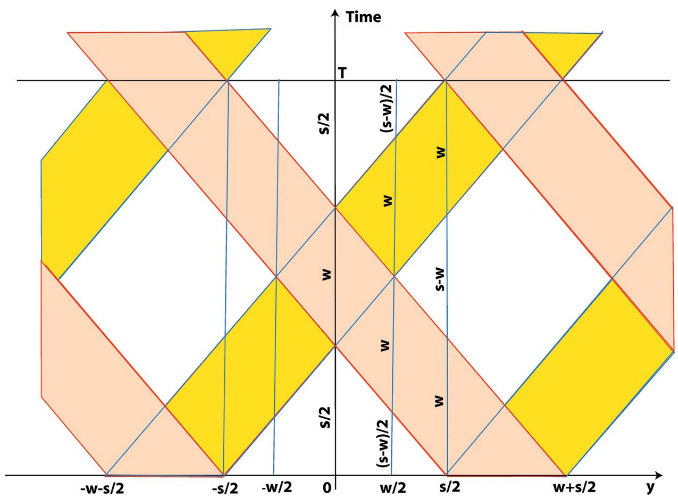

Figure 4
Time evolution of the slots (white), front walls (red) and back walls (yellow) over a time gap T from one slot to another for clockwise rotation. s and w denote the width of the slot and of the wall, and y indicates the position of the beam.

In order to trace the intensity of the beam which exits the disk we first scanned the uniformly rotating disk with a narrow beam entering the disk at the height of the center of the slots. The beam (or part of it) should pass through the disk only if it penetrates a slot both in the front and the back of the disk, without meeting any of its walls. To understand the intensity reduction of the beam by the rotating disk we diagrammatically visualize the position of the front and back slots and walls at different times. Since the slots and the walls between them are identical and the rotation is uniform, the intensity reduction is periodic. Hence, it is sufficient to consider this reduction during the time gap T from one slot to another. To simplify the analysis, without loss in generality, we scaled the unit of time to make all inclination angles to be 45° (see Fig. 4).

If the beam passes through the center of the disk (origin) the intensity entering the front of the disk is reduced by a factor $s/(s+w)$, the proportion of time in the white region in one period, where s and w denote the width of the slot and of the wall between two adjacent slots, respectively. This factor expresses the fraction of time the beam hits the slot at the entrance. Since the slots are diametrically aligned, if the beam (or part of it) passes through the center of the disk, anything entering a slot at the front of the disk will also meet a slot at its back, implying that the intensity of the beam exiting the back of the disk will be $s/(s+w)$ times its initial intensity.

If the beam does not pass through the center of the disk, part of the beam entering the front of the disk will be further obstructed by the walls at the back, implying an additional reduction in intensity. The exact dependence of the intensity of the beam on its displacement y from the center of the disk (assuming $y = 0$ at the center) is derived from Fig. 4 as follows: the intensity decreases linearly from its value $s/(s+w)$ for y = 0 to the value $(s-w)/(s+w)$ at $y = \pm w/2$ and remains at

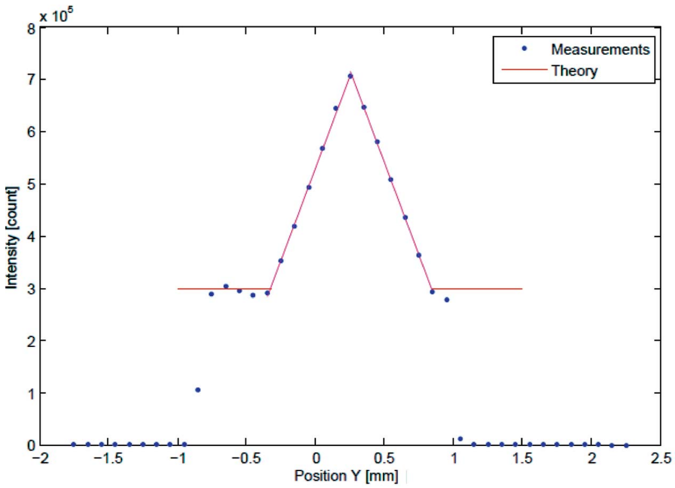

Figure 5
The y-scan and the predicted curve.

the same value until $y = \pm(s/2 + w)$. A comparison of the experimental scan with this theoretical prediction is shown in Fig. 5. The extremities of the scans are partially blocked by the openings of the vacuum chamber, as seen from the figure.

From this scan, we then perform the initial alignment by moving the rotor system to the maximum point of the scan. Using the SMS we obtain the spectrum of the absorber at low rotation frequency. The observed shift directed us to align the center of the beam to coincide with the axis of rotation. Since the alignment shift is proportional to the rotation frequency, if we begin with a high rotation the Mössbauer spectrum should run away from the (frequency) observation window. Thus, it was necessary to perform a set of scans by gradually increasing the rotation frequency. At each rotation frequency, the observed shift directed us to how to improve the alignment of the center of the beam to the axis of rotation.

In cases when the spectral widening became too large to obtain a statistically meaningful spectrum, we narrowed the effective width of the slit by rotating it. We have seen that this procedure indeed reduces the widening and increases the Mössbauer absorption effect, as predicted by the theory. For example, the spectra of two runs at the same rotation frequency 33 Hz, without (run 11) and with the slit rotated 30° (run 14), for the two states (a) and (b) described above are presented in Fig. 6. Least-squares analyses of these spectra yield the parameters listed in Table 1.

We observed that the use of the slit increased the absorption effect from 0.13 to 0.33 and reduced the line width from γ = 1.57 (8) mm s^{-1} to γ = 0.52 (5) mm s^{-1}. Even though the use of the slit reduces the count rate from 2630 counts s^{-1} (with measuring time 55 min for run 11) to 300 counts s^{-1} (with measuring time 47 min for run 14) there was no need to prolong the measuring time for a comparable quality resonant line. From Table 1 we observe that the use of the slit improved the accuracy of the fitted line parameters even with a significantly lower count rate. Note that the shifts x_0 obtained are different for the two runs. Nevertheless, in both runs similar shifts were obtained for both states (a) and (b).

Table 1
Parameters of resonant spectra for states (a) and (b) at 33 Hz rotation.

Run	Effect (%)	γ (mm s^{-1})	Shift x_0 (mm s^{-1})
11a	12.38 (41)	1.56 (09)	0.37 (05)
11b	14.12 (39)	1.59 (08)	0.37 (05)
14a	32.04 (2.17)	0.52 (05)	1.42 (03)
14b	33.58 (2.40)	0.53 (05)	1.41 (04)

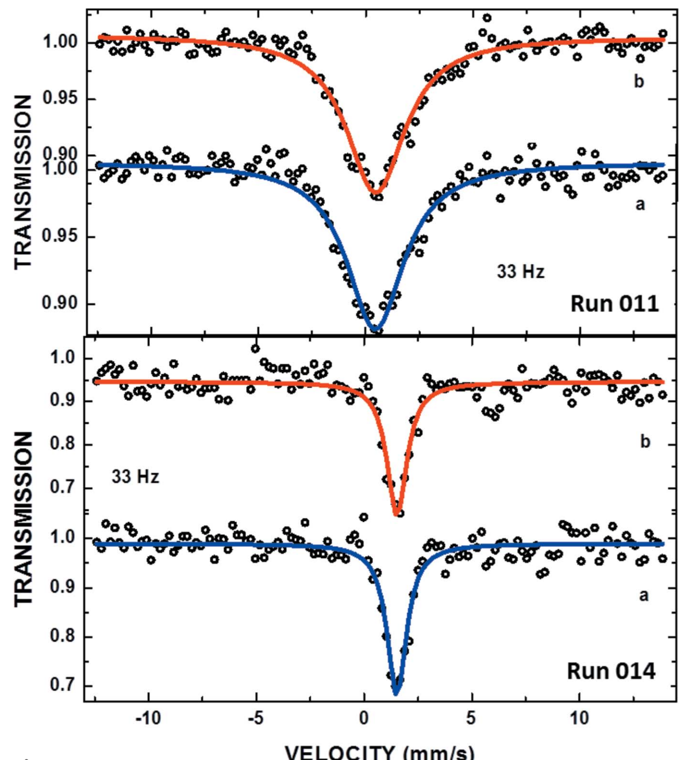

Figure 6
Absorption spectra, converted to average linear velocity form, for states (a) and (b) at 33 Hz rotation. Run 11 (top) without the slit and run 14 (bottom) with the slit.

3. The relative spectral shift

During each run we obtained a spectral curve for each of the above-mentioned states (a) and (b) and calculated the *relative shift* by subtracting the shift of the parallel state (b) from that of the anti-parallel state (a). For example, the relative shift for run 11 is 0.00 (7) and for run 14 is 0.01 (4), see Table 1. The relative shift remained negligible at higher rotation frequencies up to 100 Hz.

On the other hand, at 100 Hz we observed the first non-trivial relative shift of 0.16 (8) mm s^{-1}, as shown in Fig. 7 and Table 2.

At a rotation frequency of 200 Hz, in two sequent runs 31 and 32 of about 6 h each, the relative shift was significantly increased as shown in Fig. 8 and Table 3. Table 3 presents the parameters of these spectra including the vibration shift calculated by the method given by Friedman *et al.* (2016).

The table reveals that in these runs the measured shift for each state differs from run to run (probably due to the alignment) but the relative shift nevertheless remained almost constant for both runs. This indicates that the relative shift is

Table 2
Parameters of resonant spectra for states (*a*) and (*b*) at 100 Hz rotation.

Run	Effect (%)	γ (mm s^{-1})	Shift x_0 (mm s^{-1})
16*a*	15.11 (76)	1.24 (10)	−1.04 (06)
16*b*	19.24 (82)	1.25 (08)	−1.20 (05)

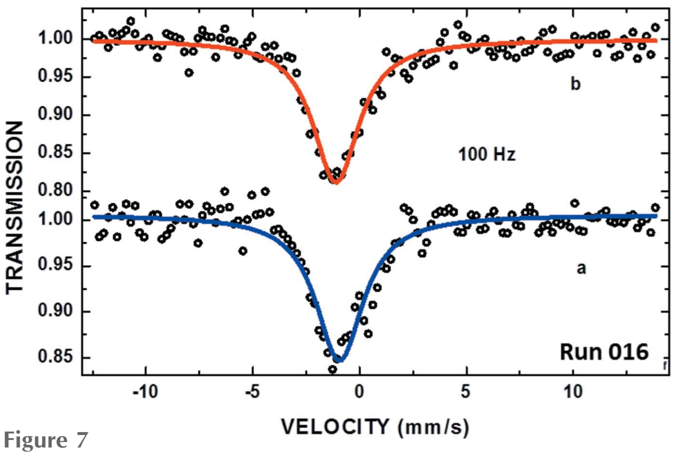

Figure 7
Absorption spectra, converted to average linear velocity form, for states (*a*) and (*b*) at 100 Hz rotation.

not sensitive to the alignment of the system, as it was expected. Moreover, the observed relative shift was at least one order of magnitude higher than the vibration shift (high signal-to-noise ratio), as discussed later, hence it can be used to claim conclusive evidence. This suggests that the actual relative shift at 200 Hz in our setup is approximately 0.41 (14) mm s^{-1}.

We expect the relative shift to be proportional to the square of the rotation frequency. Thus, for a rotation at 100 Hz we expect this shift to be one-quarter of the shift at 200 Hz, which is consistent with the relative shift obtained in run 16 at 100 Hz (Fig. 8 and Table 3). For lower rotation frequencies the observed relative shift was less than the accuracy of our measurements, as expected. Further runs in both directions at 300 Hz produced, as expected, an even larger relative shift. However, the very high vibrations in these runs made these runs inconclusive.

The relative shifts caused by vibrations were calculated according to the formula derived by Friedman *et al.* (2016). We found that the impact of vibrations for rotation frequencies below 200 Hz, inclusive, are relatively negligible, see Table 3. However, at 300 Hz their impact is very large. This can be seen from Fig. 9 which compares the radial velocities $v_r(\varphi)$ caused by the bearing system at different points φ of the disk at 200 Hz and 300 Hz. The spectral shift due to vibrations in states (*b*) and (*a*) is the average of $v_r(\varphi)$ in the intervals $[0, 180^\circ]$ and $[180^\circ, 360^\circ]$, respectively.

The figure reveals that the radial velocities at 200 Hz are significantly smaller than those at 300 Hz. Moreover, at 200 Hz these velocities are balanced over these two intervals, implying a significantly low relative shift due to vibrations.

The existence of the statistically significant, almost constant, non-zero actual relative shift for two runs at 200 Hz indicates the effect of acceleration on the absorption resonant line and hence on time dilation.

Table 3
Parameters of resonant spectra and the vibration shifts for states (*a*) and (*b*) at 200 Hz rotation.

Run	Effect (%)	γ (mm s^{-1})	Shift x_0 (mm s^{-1})	Vibration shift (mm s^{-1})
31*a*	6.68 (18)	3.29 (24)	−0.58 (11)	−0.007
31*b*	8.01 (27)	3.14 (22)	−1.01 (09)	0.007
32*a*	7.29 (20)	3.25 (20)	−0.22 (12)	−0.01
32*b*	8.31 (29)	3.13 (21)	−0.61 (09)	0.01

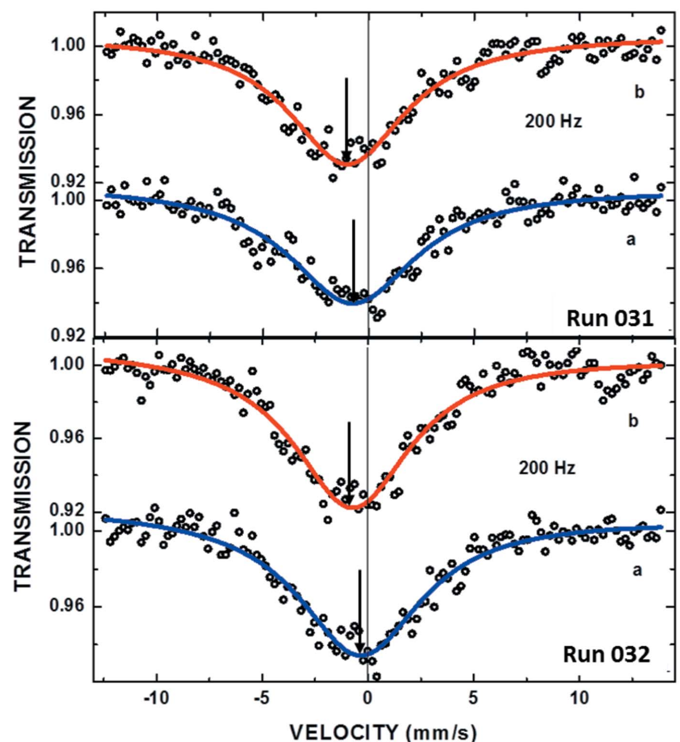

Figure 8
Absorption spectra, converted to average linear velocity form, of run 31 (top) and 32 (bottom) for states (*a*) and (*b*) at 200 Hz rotation.

Currently the only relativistic model that predicts a non-zero relative shift in such an experiment is the 'universal maximal acceleration' model (Friedman & Gofman, 2010; Friedman, 2011). Based on this model, the relative shift s_r (in m s^{-1}) is given by $s_r/c = 2\omega^2 r/a_m$, where c is the speed of light (in m s^{-1}), ω is the rotation frequency (in rad s^{-1}), r is the

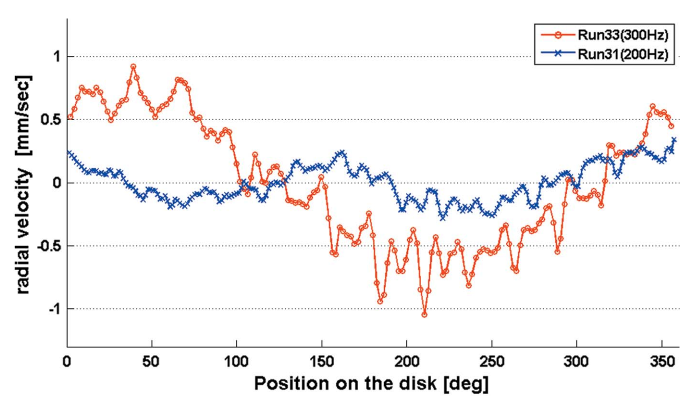

Figure 9
Comparison of vibrations at 200 Hz and 300 Hz rotation.

radius of the disk (in m), which was $r = 0.05$ m, and a_m is the postulated universal maximal acceleration (in m s^{-2}). Based on our findings at 200 Hz, this model predicts

$$a_m = \frac{2(2\pi \times 200)^2 \times 0.05 \times 3 \times 10^8}{0.41 \times 10^{-3}} = 1.2 \times 10^{17}\ \mathrm{m\,s^2}. \quad (1)$$

This value for a_m seems to be too low for a universal maximal acceleration $a_m = 10^{19}$ m s^{-2} which was based on Kündig's experiment (Kündig, 1963).

In a current paper (Potzel, 2016), Potzel used this model and results of high-resolution 93.3 keV Mössbauer resonance in ^{67}ZnO and β'-brass to test the clock hypothesis. He came up with a lower limit of $a_m > 1.5 \times 10^{21}$ m s^{-2}, higher than the ones above. Also Schuller (2002) predicted a lower bound for maximal acceleration, $a_m > 10^{22}$ m s^{-2}. This may be an indication that the maximal acceleration affecting time dilation may be not universal, and may depend on different physical situations, as explained by Caianiello (1981).

4. Discussion and conclusions

The main objective of this research is to explore the effect of acceleration on time dilation. The time dilation is measured by the shift in the Mössbauer resonant line of an accelerated absorber. The acceleration of the absorber was generated by rotating it using a rotor system. For technical reasons an appropriate resonant line could be obtained only with the use of a synchrotron Mössbauer source. Using the setup diagrammatically presented in Fig. 2 we separated the absorption of a rotating absorber into two states (*a*) and (*b*) when the acceleration is anti-parallel and parallel to the SMS radiation, respectively, and obtained the absorption lines for each state. Since the absorption lines for each of the states are generated by the same source and absorber, and are equally affected by the velocity of the absorber with respect to the source, these two spectra should be identical without the influence of acceleration on time.

In this follow-up experiment we managed to increase significantly the count rate to obtain spectra at higher rotation frequencies and to monitor the vibrations of the rotor/bearing system. We found (i) a fast way for the initial alignment of the beam to the center of the disk by observing a vertex at the center of the disk while scanning the disk perpendicular to the direction of the beam, (ii) a way to monitor vibrations by the use of an electronic control system and (iii) a method to quantify the effects of non-random vibrations on the spectral shift. The effect of non-random vibrations on the spectral shift cannot be overlooked in any experiment testing time dilation, as it identifies whether the observed spectral shift is conclusive in each run.

The experiment revealed that within the given setup and rotation frequencies of 200 Hz and higher the resonant shifts of the two states are not the same. We observed a stable statistically significant non-zero relative shift between the spectral lines in the two states. In particular, for two long runs at 200 Hz in which the effect of vibrations was negligible, the almost constant relative shift of about 0.41 (14) mm s^{-1} indicates the effect of acceleration on time dilation (see Fig. 8 and Table 3). A hint of the influence of acceleration on time dilation was already observed at 100 Hz rotation.

The 'universal maximal acceleration' model, the only theoretical model available nowadays that predicts such a non-zero relative shift, yields an estimate of $a_m = 1.2 \times 10^{17}$ m s^{-2} for the maximal acceleration based on the results of this experiment. Surprisingly, this value for a_m seems to be too low for a universal maximal acceleration $a_m = 10^{19}$ m s^{-2} based on Kündig's experiment (Kündig, 1963) and certainly lower that the limits set by Potzel (2016) and Schuller (2002).

This discrepancy indicates that the maximal acceleration depends on the physical situation, or the need for another model to explain the non-zero relative shift. In order to better understand the relative spectral shift due to rotation we plan to repeat the experiment this summer at ESRF with an improved setup to further increase the count rate, to reach higher rotation frequencies and to control and minimize the effect of vibrations.

Acknowledgements

We wish to acknowledge the financial support of the Jerusalem College of Technology and ESRF. Special thanks to Eng. O. Efrati, Eng. T. Frumson, Eng. A. Finkelstein from Colibri Spindles Ltd for upgrading the rotor system, and Eng. Z. Brand, Eng. N. Levi, Eng. I. Shafir from Nuclear Research Center-Negev for designing the mechanical components, Eng. M. Friedman for his help with the optical sensor, Dr M. Manevich and Y. Varshal of Jerusalem College of Technology for help with the slit and its holder, and Dr S. Eliav from the Nano Center of the Hebrew University who managed to grow the slit.

References

Caianiello, E. R. (1981). *Lett. Nuov. Cim.* **32**, 65.
Einstein, A. (1905). *Ann. Phys.* **17**, 89.
Einstein, A. (1911). *Ann. Phys.* **340**, 898–908.
Friedman, Y. (2011). *Ann. Phys.* **523**, 408–416.
Friedman, Y. (2013). *J. Phys. Conf. Ser.* **437**, 012017.
Friedman, Y. & Gofman, Yu. (2010). *Phys. Scr.* **82**, 015004.
Friedman, Y. & Nowik, I. (2012). *Phys. Scr.* **85**, 065702.
Friedman, Y., Nowik, I., Felner, I., Steiner, J. M., Yudkin, E., Livshitz, S., Wille, H.-C., Wortmann, G., Arogeti, S., Levy, R., Chumakov, A. I. & Rüffer, R. (2016). *Europhys. Lett.* **114**, 50010.
Friedman, Y., Yudkin, E., Nowik, I., Felner, I., Wille, H.-C., Röhlsberger, R., Haber, J., Wortmann, G., Arogeti, S., Friedman, M., Brand, Z., Levi, N., Shafir, I., Efrati, O., Frumson, T., Finkelstein, A., Chumakov, A. I., Kantor, I. & Rüffer, R. (2015). *J. Synchrotron Rad.* **22**, 723–728.
Kirkpatrick, P. & Baez, A. V. (1948). *J. Opt. Soc. Am.* **38**, 766–774.
Kündig, W. (1963). *Phys. Rev.* **129**, 2371–2375.
Potapkin, V., Chumakov, A. I., Smirnov, G. V., Celse, J.-P., Rüffer, R., McCammon, C. & Dubrovinsky, L. (2012). *J. Synchrotron Rad.* **19**, 559–569.
Potzel, W. (2016). *Hyperfine Interact.* **237**, 38.
Rüffer, R. & Chumakov, A. I. (1996). *Hyperfine Interact.* **97–98**, 589–604.
Schuller, F. P. (2002). *Phys. Lett. B*, **540**, 119–124.